Proceedings of Meetings on Acoustics

Volume 19, 2013 http://acousticalsociety.org/

ICA 2013 Montreal
Montreal, Canada
2 - 7 June 2013

Underwater Acoustics
Session 2pUWa: Ocean Ambient Noise

2pUWa9. Model for underwater noise radiated by submerged wind turbine towers

Todd A. Hay*, Yurii A. Ilinskii, Evgenia A. Zabolotskaya and Mark F. Hamilton

***Corresponding author's address: Applied Research Laboratories, The University of Texas at Austin, 10000 Burnet Rd., Austin, TX 78713-8029, hayta@arlut.utexas.edu**

Sustained tonal noise radiated by towers supporting offshore wind turbines contains energy in frequency bands that may disturb marine mammals, or interfere with passive sonar and seismic sensors and underwater communication equipment. Understanding the generation and propagation of underwater noise due to the operation of wind farms is important for determining strategies for mitigating the environmental impact of these noise sources. An analytic model based on a Green's function approach was previously developed for the sound radiated in the water column by a pulsating cylindrical structure embedded in horizontally stratified layers of viscoelastic sediment [Hay et al., J. Acoust. Soc. Am. 130, 2558 (2011)]. This model has since been adapted to include relaxation and viscous losses in seawater and empirical loss factors for the sedimentary layers. For propagation over range-dependent environments the analytic model has been coupled to a parabolic equation code. Simulations are presented for several bathymetries, sediment types, and tower array configurations. [Supported by Department of Energy DE-EE0005380]

Published by the Acoustical Society of America through the American Institute of Physics

 [DOI: 10.1121/1.4800571]
Received 22 Jan 2013; published 2 Jun 2013

INTRODUCTION

Recent proposals to install offshore wind farms in the coastal waters of the United States has generated interest in understanding the noise that would be generated by the vibrations of the wind turbine support structures. A model has been developed for the purposes of assessing the impact that this underwater noise would have on acoustic communication systems, seismic sensors, and marine mammals.

THEORY

Here we present a model for the sound radiated by arrays of pulsating cylindrical towers or piles immersed in water and embedded in layers of viscoelastic sediment. The cylinder is modeled as an ensemble of independent volume sources arranged in a vertical line and positioned in the water column and sediment along the z axis. The air, water and sediment layers are assumed to be infinite in the x-y plane but have finite thicknesses along the z axis with boundaries at $z = z_j$. The layers have densities ρ_j, longitudinal sound speeds $c_{l,j}$, transverse sound speeds $c_{t,j}$, shear moduli μ_j, shear viscosities η_j, and dilitational viscosities ζ_j.

The Green's function for displacement $\mathbf{u}$ is derived by considering the momentum equation for an isotropic, viscoelastic medium

$$\left(\lambda + \zeta\frac{\partial}{\partial t} + \mu + \eta\frac{\partial}{\partial t}\right)\nabla\nabla\cdot\mathbf{u} + \left(\mu + \eta\frac{\partial}{\partial t}\right)\nabla^2\mathbf{u} = \rho\frac{\partial^2\mathbf{u}}{\partial t^2}, \tag{1}$$

where $\lambda = \rho c_l^2$ is a Lamé parameter. The Green's function $\mathbf{g}$ for displacement at a location $\mathbf{r}$ in the j^{th} layer due to a point volume source located at $\mathbf{r}_0$ also within the j^{th} layer, and pulsating with time dependence $e^{-i\omega t}$, satisfies

$$\left(\hat{\lambda}_j + \hat{\mu}_j\right)\nabla\nabla\cdot\mathbf{g} + \hat{\mu}_j\nabla^2\mathbf{g} + \rho\omega^2\mathbf{g} = s\nabla\delta(\mathbf{r} - \mathbf{r}_0), \tag{2}$$

where $\hat{\lambda}_j = \lambda_j - i\omega\zeta_j$, and $\hat{\mu}_j = \mu_j - i\omega\eta_j$ are the complex Lamé parameters, $\lambda_j = \rho c_{l,j}^2$, and s is the source strength [related to the volume velocity Q by $s = -(\rho c_{l,j}^2/i\omega)Q$]. [1] At points $\mathbf{r}$ outside the j^{th} layer the Green's function satisfies

$$\left(\hat{\lambda}_k + \hat{\mu}_k\right)\nabla\nabla\cdot\mathbf{g} + \hat{\mu}_k\nabla^2\mathbf{g} + \rho\omega^2\mathbf{g} = \mathbf{0}, \tag{3}$$

where $k \neq j$ is the index of the layer in which $\mathbf{r}$ lies. Boundary conditions requiring continuity of displacement and stress are imposed at each interface. Due to symmetry the Green's function is a function of depth z and range R only, where $R^2 = x^2 + y^2$. Therefore it may be decomposed into its angular spectrum in the x-y plane. [1] Once the boundary conditions are satisfied (see [1] for details) the pressure at some point $\mathbf{r} = (R, z)$ in layer k due to a source located at $\mathbf{r}_0 = (0, z_0)$ in layer j may be expressed in terms of the inverse Hankel transform:

$$P(\omega, \mathbf{r}) = -\frac{\rho_k\omega^2}{2\pi}\int_0^\infty s(z_0)\Psi(z, z_0, \kappa_{l,j}, \kappa_{t,j}, \kappa_{l,k}, \kappa_{t,k})J_0(\kappa R)\,d\kappa, \tag{4}$$

where Ψ is the angular spectrum of the displacement potential, and the displacement potential ψ is related to the Green's function by $\mathbf{g} = \nabla\psi$. The z axis components of the wavenumbers of the longitudinal and transverse waves are

$$\kappa_{l,j} = \sqrt{\kappa^2 - k_{l,j}^2}, \qquad \kappa_{t,j} = \sqrt{\kappa^2 - k_{t,j}^2}, \tag{5}$$

where $k_{l,j}^2 = \omega^2/c_{l,j}^2$, $k_{t,j} = \omega^2/c_{t,j}^2$, and

$$c_{l,j} = \sqrt{\frac{\hat{\lambda}_j + 2\hat{\mu}_j}{\rho_j}}, \qquad c_{t,j} = \sqrt{\frac{\hat{\mu}_j}{\rho_j}}, \tag{6}$$

are the longitudinal and transverse sound speeds, respectively, in the j^{th} layer (and similarly for the k^{th} layer). Alternatively, the wavenumbers $k_{l,j}$ and $k_{t,j}$ may be expressed in terms of loss factors $\alpha_{l,j}$ and $\alpha_{t,j}$ as

$$k_{l,j} = \omega\sqrt{\frac{\rho_j}{\lambda_j + 2\mu_j}}\left(1 + i\frac{\alpha_{l,j}}{2\pi}\right), \qquad k_{t,j} = \omega\sqrt{\frac{\rho_j}{\mu_j}}\left(1 + i\frac{\alpha_{t,j}}{2\pi}\right), \tag{7}$$

where $\alpha_{l,j}$ and $\alpha_{t,j}$ are loss factors for longitudinal and transverse waves, respectively, in the j^{th} layer expressed in Np/wavelength. Expressing the sound speeds in this way allows experimentally observed loss factors to be used.

The sound pressure from a pulsating cylindrical structure coincident with the z axis and extending from $z = z_{\min}$ to $z = z_{\max}$ may be calculated by integrating Eq. (4) along the length of the structure, i.e.,

$$P_{\text{cyl}}(\omega, \mathbf{r}) = -\frac{\rho_k \omega^2}{2\pi}\int_{z_{\min}}^{z_{\max}} \tilde{s}(z_{\text{src}})\, dz_{\text{src}} \int_0^{\infty} \Psi(z, z_0, \kappa_{l,j}, \kappa_{t,j}, \kappa_{l,k}, \kappa_{t,k}) J_0(\kappa R)\, d\kappa, \tag{8}$$

where $\tilde{s}$ is the source strength per unit length.

Due to linear superposition, the pressure field produced by arrays of pulsating wind turbine towers may be modeled by simply adding the individual contributions of each tower. If the towers are assumed to share the same source strength function $\tilde{s}$ then Eq. (8) must only be evaluated once, and the total field is found simply by moving the origin to each tower location, interpolating the pressure field onto a fixed grid, and summing, i.e.,

$$P_{\text{array}}(\omega, \mathbf{r}) = \sum_{j=1}^{N} e^{i\phi_j} P_{\text{cyl}}(\omega, \mathbf{r} - \mathbf{r}_j), \tag{9}$$

where $\mathbf{r}_j = (x_j, y_j, z)$ and (x_j, y_j) is the location of the j^{th} tower in the x-y plane, and ϕ_j is the pulsation phase of the j^{th} tower. For incoherent pulsation ϕ_j is a random number chosen from some distribution and is unique to the j^{th} tower, while for coherent pulsation the phase factor ϕ_j is constant.

Range-dependent propagation

While the model described in the previous section is only valid for range-independent environments, pressure fields calculated with Eq. (8) may be coupled to a parabolic equation code to simulate propagation over range-dependent bathymetries with depth- and range-dependent sound speeds. [2] For these purposes a modified version of the range-dependent acoustic model (RAM) was implemented. [3]

SIMULATIONS

We now present simulations for a cylindrical wind turbine tower with radius R_0 of 1 m. We assume that the tower is immersed in a water column of height 25 m, and is embedded 15 m into the sediment. Measurements taken on the support structures of an operational wind farm suggest that the radial acceleration of the tower surface a in air is roughly constant with frequency (except at frequencies near gear box resonances) and is nominally 2 mm/s^2. [4]

Due to lack of measurements of the tower acceleration in water or sediment we will assume that the tower pulsates uniformly along its entire length with surface acceleration $a_0 = 2$ mm/s^2. Therefore the volume velocity per unit length is $i2\pi R_0 a_0/\omega^2$ and $\tilde{s}(z_{\text{src}}) = 2\pi R_0 \rho_j c_{l,j}^2 a_0/\omega^3$. However, the portions of the tower in the water column and sediment would likely be pulsating

with a lower amplitude relative to the portion in air, due to loading by the surrounding media. Therefore these simulations of the pressure in the water column should be considered to be an upper bound of what may realistically be expected.

Two types of ocean bottom will be investigated. The first is silt sediment, which has relatively high losses. Its parameters are ρ =1700 kg/m^3, $c_l = 1700$ m/s, $c_t = 80\tilde{z}^{0.3}$, $\alpha_l = 0.115$ Np/wavelength, and $\alpha_t = 0.173$ Np/wavelength, where $\tilde{z}$ is the depth referenced from the water-sediment interface. The second bottom type considered here is basalt which has material properties $\rho = 2700$ kg/m^3, $c_l = 5250$ m/s, c_t =2500 m/s, $\alpha_l = 0.012$ Np/wavelength and $\alpha_t = 0.024$ Np/wavelength. [2]

Figures 1 and 2 show the pressure (expressed in dB re 1 μPa) due to pulsations of the portions of the tower in the water column [parts (a)], the sediment [parts (b)], and the total field [parts (c)] for silt and basalt ocean bottoms, respectively, at a frequency of 1000 Hz. The horizontal dashed white line shows the location of the interface between the water and the ocean bottom at a depth of 25 m.

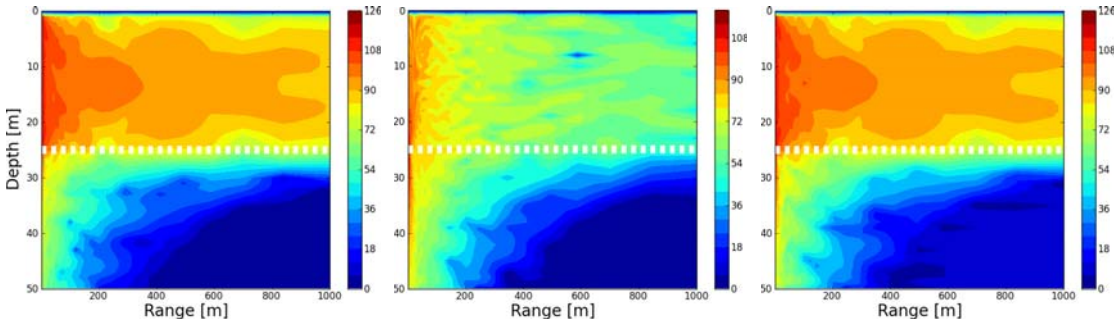

(A) Tower portion in water **(B)** Tower portion in sediment **(C)** Total field

FIGURE 1: Pressure field (dB re 1 μPa) with silt bottom at 1000 Hz.

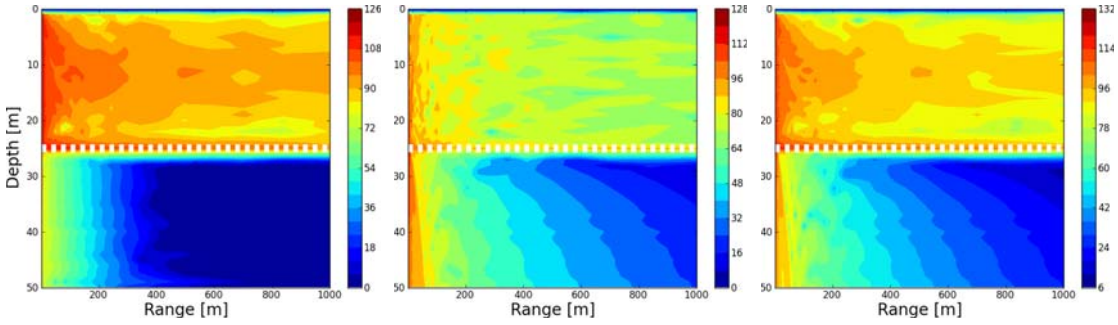

(A) Tower portion in water **(B)** Tower portion in sediment **(C)** Total field

FIGURE 2: Pressure field (dB re 1 μPa) with basalt bottom at 1000 Hz.

Note that for both ocean bottom types the pressure is zero at the surface due to the pressure release condition, and for the hard basalt bottom (Fig. 2) the pressure is higher at the interface between the water and the sediment at $z = 25$ m. This is due to fact that the impedance (ρc_l) of the basalt is much greater than that of the water and the effect is absent in Fig. 1 because the impedance of silt is much closer to that of water. Also note that the overall pressure levels are higher with the basalt bottom, due to the lower losses.

We next show the dependence of the pressure field at a fixed depth of 12.5 m (half the water column depth) at five logarithmically spaced frequencies between 10 and 1000 Hz to distances up to 100 km from the pulsating tower. Figure 3(a) shows the pressure field for sediment

composed of silt while part (b) shows the field for a basalt ocean bottom. Note that the pressure levels for the basalt case are higher overall, especially at large ranges.

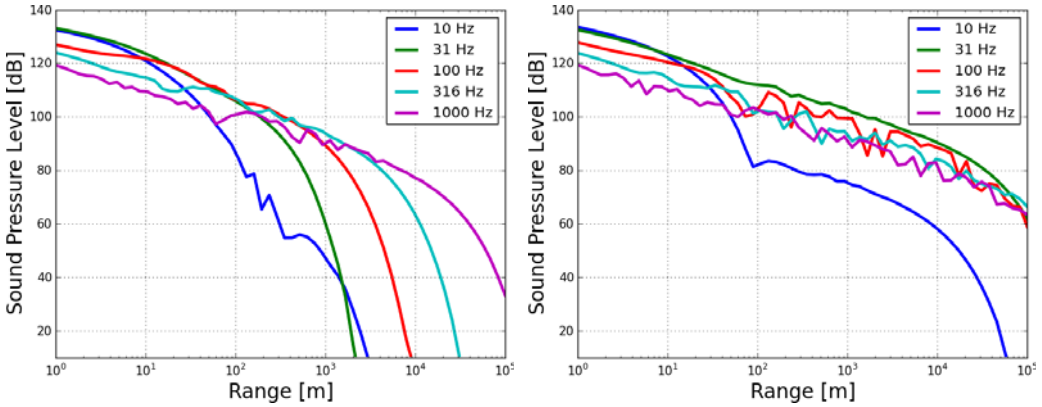

(A) Silt sediment **(B)** Basalt sediment

FIGURE 3: Pressure field (dB re 1 μPa) at z = 12.5 m.

Arrays of towers

Figure 4 shows the pressure field given by Eq. (9) with range at a depth of $z = 12.5$ m for (a) a single turbine tower, (b) an array of 10 towers spaced 1 km apart along the x axis, (c) a 10x10 array (with the same 1 km spacing) of 100 pulsating towers. In all cases the frequency is 316 Hz. The black dots in Fig. 4 indicate the locations of the towers. The random phase variable ϕ_j was chosen from the uniform distribution $U(0, 2\pi)$. Note that as more towers are added the pressure field does change but the maximum pressure at the center of the array remains roughly constant.

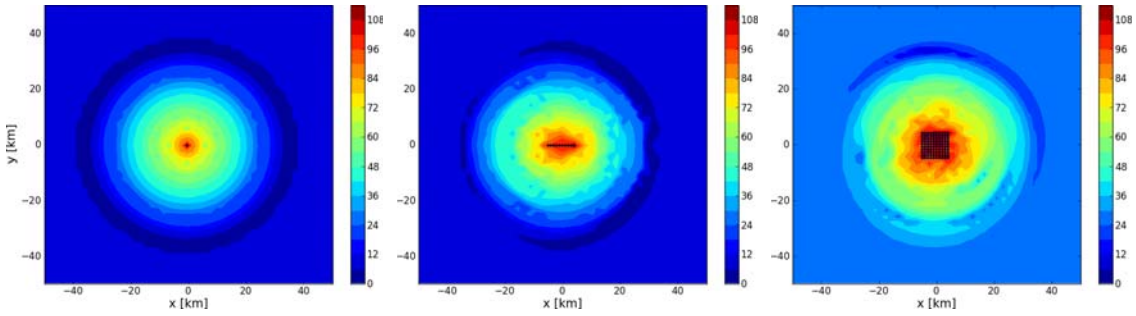

(A) Single tower **(B)** 10x1 array of towers **(C)** 10x10 array of towers

FIGURE 4: Pressure field (dB re 1 μPa) at $z = 12.5$ m at a frequency of 316 Hz.

Range dependence

To illustrate propagation in range-dependent environments the sound field predicted by Eq. (8) at a range of 55 km was coupled to a version of RAM modified to account for interaction with a sediment bottom. [3] The parabolic equation model was then used to propagate the sound field from a range of 55 km out to 200 km over a bathymetry which varies with range and sound speed which varies with depth. The two sound speed profiles considered here are shown in Fig. 5(a). The blue curve is the Munk profile, an idealized profile for a temperate ocean, [5] while

the green curve is an idealization of a polar ocean profile. Parts (b) and (c) of Fig. 5 show the pressure field for the two different sound speed profiles at a frequency of 1000 Hz and a silt sediment bottom. The interface between the water and the sediment is shown by the dashed white line.

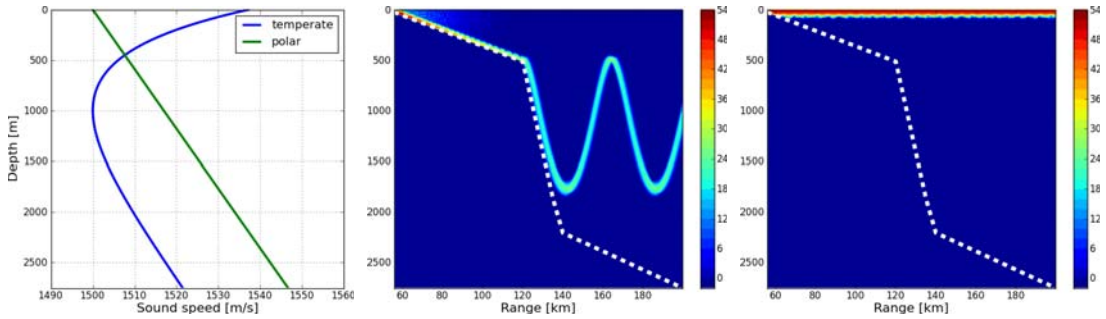

(A) Sound speed profile **(B)** Pressure field in temperate ocean **(C)** Pressure field in polar ocean

FIGURE 5: Sound speed profiles and pressure fields (dB re 1 μPa) for propagation over a range-dependent environment at 1000 Hz.

In the case of the temperate ocean profile [Fig. 5(b)] the sound is refracted downward and bounces off the ocean bottom repeatedly until the steep drop at a range of 120 km is reached. At this point the sound is alternatively refracted upward and downward about the depth of minimum sound speed (1 km). The pressure field for the polar ocean profile in part (c) is qualitatively different. Here the sound is refracted upward and reflects from the air-water interface. While each bounce from the ocean bottom attenuates the sound pressure significantly, the air-water interface is modeled here as a perfect reflector and so the pressure is not reduced with each bounce from the air-water interface.

SUMMARY

A semi-analytic Green's function model was developed for underwater noise due to pulsating towers supporting offshore wind turbines. Simulations of the sound radiated in the water column by a these towers embedded in horizontally stratified layers of viscoelastic sediment were presented. For long-range propagation over range-dependent environments the semi-analytic model was coupled to a parabolic equation code, and simulations showing qualitatively different results were discussed.

ACKNOWLEDGMENTS

This research was supported by Department of Energy grant number DE-EE0005380.

REFERENCES

[1] T. A. Hay, Yu. A. Ilinskii, Z. A. Zabolotskaya, and M. F. Hamilton, "Model for bubble pulsation in liquid between parallel viscoelastic layers", J. Acoust. Soc. Am. **132**, 124–137 (2012).

[2] F. B. Jensen, W. A. Kuperman, M. B. Porter, and H. Schmidt, *Computational Ocean Acoustics*, 2nd edition (Springer-Verlag, New York, NY (USA)) (2011).

[3] M. D. Collins, “A split-step Padé solution for the parabolic equation method”, J. Acoust. Soc. Am. **93**, 1736–1742 (1993).

[4] Ingemansson Technology AB, “Utgrunden off-shore wind farm - measurements of underwater noise”, Technical Report, Ingemansson Technology AB (2003).

[5] W. H. Munk, “Sound channel in an exponentially stratified ocean, with application to SOFAR”, J. Acoust. Soc. Am. **55**, 220–226 (1973).